



ARTICLE

Study of Spectral Response Characteristics of Oilseed Rape (*Brassica napus*) to Particulate Matters Based on Hyper-Spectral Technique

Lijuan Kong^{1,2}, Haiye Yu^{1,2}, Zhaojia Piao^{1,2}, Meichen Chen^{1,2}, Jingmin Dang¹, Lei Zhang^{1,2} and Yuanyuan Sui^{1,2,*}

¹College of Biological and Agricultural Engineering, Jilin University, Changchun, 130022, China

²The Key Laboratory of Bionic Engineering (Ministry of Education, China), Jilin University, Changchun, 130022, China

*Corresponding Author: Yuanyuan Sui. Email: suiyuan@jlu.edu.cn

Received: 07 September 2020 Accepted: 18 December 2020

ABSTRACT

Haze is mainly caused by the suspended particulate matters in the air, of which the particulate matters pollution harms leaf vegetables. In this paper, oilseed rapes at four different growing periods were investigated in a simulated particulate pollution environment. In combination of hyper-spectral technology and micro examination, the response of hyper-spectral characteristics of the leaf to particulate matters was investigated in-depth. The hyper-spectral, chlorophyll content, net photosynthetic rate and stomatal conductance of leaf were obtained. The deposition and adsorption of particulate matters on the leaf were observed by Environmental Scanning Electron Microscope (ESEM). Normalized difference vegetation index (NDVI), modified red edge normalized (mNDVI705) and modified red edge simple ratio index (mSR705) were selected as characteristic parameters and the range of 510 nm~620 nm as the sensitive band. 16 methods were used to establish the physiological information inversion model. The main results were as follows: Under the influence of particulate matters, the spectral reflectance decreased as a whole. With the increase of leaf age, the phenomenon of blue shift aggravated. The amplitude of yellow and blue edge decreased with overall decreasing vegetation indices. The furrows and irregular band protrusions in leaves were favorable for keeping particulate matters. With longer affecting time and more deposition of particle matters on the leaf, the stomatal opening became smaller. After comparing, principal component regression (PCR) + multiple scatter correction (MSC) + second derivative (SD) + Savitzky-Golay smooth (SG), and partial least square (PLS) + multiple scatter correction (MSC) + first derivative (FD) + Savitzky-Golay smooth (SG) were determined the best method to establish the inversion model of chlorophyll content and net photosynthetic rate respectively. This study may bring novel ideas for the diagnosis and analysis of the physiological response of leaf vegetables under particulate matters pollution using hyper-spectral technology.

KEYWORDS

Particulate matter; hyper-spectral technique; oilseed rape; chlorophyll content; net photosynthetic rate; stomata; inversion model

1 Introduction

Haze has always been one of the most intractable air pollution issues, which is primarily caused by suspended particulate matters in the air. Particulate matter (PM) pollution not only affects human life, but



also influences the growth of plants. Particulate matter inhibits the photosynthesis of vegetables, resulting in a decrease of vegetable quality and yield [1]. Moreover, carrying poisonous and harmful substances such as heavy metals and organic pollutants, particulate matters enter into the soil through atmospheric deposition or accompanied with rain and snow. After being absorbed in the circulation of vegetables, particulate matters cause great danger to the human when vegetables are consumed, which destroys the ecosystem of soil-crop-consumers. Studies have shown that urban vegetation can absorb particulate matters, which is beneficial to reducing harmful substances in the air, such as particulate matters. Plant species that are more beneficial to air purification can be screened out through their different responses to particulate matters. Most studies focus on the effect of particulate matters on trees, shrubs, and green vegetation under the condition of natural haze [2–4]. Few studies have investigated the pollution effect of haze on vegetables. Meanwhile, most of them were qualitative without advanced techniques for detection and analysis of the pollution mechanism. Moreover, natural haze occurs randomly with the difficulty of controlling test variables, long and unstable test cycles, and low repeatability. The concentration and composition of haze differ with geography, season, and weather conditions, which limits the possibility of using natural haze as experiment conditions [5]. Some researchers have simulated the occurrence of particulate matters by fuel combustion [6] and emission of collected particulate matters from wind tunnel [7]. It helps the study of the effect of particulate matters on plant appearance information, leaf physiology and ecology, and spectral characteristics by solving the problem of artificial simulation of haze environment in the lab. The occurrence of particulate matters was simulated. The effect of particulate matters on oilseed rapes during four different growing periods was investigated under the simulated particulate matter in this paper.

The change of vegetables after being subjected to particulate matters pollution cannot be observed by naked eye obviously. Although the mass of retained particulate matters on leaf surface can be measured through washing with water and weighing, the method is tedious, and the results of membrane filtration have significant errors. Moreover, some particulate matters enter the epicuticular wax, of which the amount cannot be measured by washing and weighing [8,9]. Therefore, these approaches involve destructive methods, entail time- and labour-consuming processes and require specialized skills. It is not easy or accurate to compare the influence of particulate matters pollution.

Advancements in agricultural technology have provided a reliable method for the non-destructive of plant through spectroscopy. With the fast, non-destructive and accurate characteristics, spectral technology has been widely applied in the field of plant physiological detection, environmental stress and precision agriculture, which provides a novel technology for the monitoring the difference of spectral information affected by particulate matters pollution [10,11]. The hyper-spectral characteristics of vegetation leaves are related to the vegetation and its surrounding environment. When plants are polluted under particulate matter environment, the photosynthetic characteristics and physiological information inside the plants change and the spectral characteristics also change accordingly. The spectral characteristics changes because of the changed physiological information under particulate matters. It is of great significance to analyze such changes by using hyper-spectral technology. By comparing the spectral information of healthy leaves and leaves affected by particulate matters, then analyzing the spectrum changes after particulate matters, the damage of vegetables can be identified. It provides a new method for the identification and early warning of disease of vegetables in the agricultural facility [12].

The aims of this study were as follows: Establish the physiological information inversion model considering the environment with particulate matters pollution; obtain the inversion model of leaves using a simpler and more accurate method; and meanwhile obtain the hyper-spectral response rule of leaves; and analyze the physiological changes of leaves, especially the stomata in the case of particulate matters. In the paper, based on hyper-spectral technology, hyper-spectral, first derivative spectral and physiological information such as chlorophyll content, net photosynthetic rate and stomatal conductance of the healthy leaf and the leaf affected by particulate matters during four different growing periods were compared. The

aim of the study was to obtain the spectrum response mechanism and law of oilseed rape to particulate matters during four growing periods. Micro-structural characteristics of the leaf surface, such as grooves, folds, stomata, flocculent protuberance, micro-roughness, fuzz, wax and secretory products, are essential factors affecting the retention and adsorption of particulate matters [13]. Studies have shown that, generally, with the rougher surface of plant leaves, denser grooves, and more waxy and mucus, the retention and adsorption of particulate matters will be better. On the other hand, the smooth surface of leaves with no obvious fluctuation, wide gullies, shallow and sparse grooves, and well-arranged stomata has the relatively weak ability of retention and absorption of particle matters [14–16]. The mechanism of the effect of particulate matters on leaf was analyzed in combination with the microstructural observation of ESEM. The inversion model of chlorophyll content and net photosynthetic rate in oilseed rape during the collecting period was also established respectively within the range of sensitive spectral and the modeling was optimized. The optimized inversion model could be used to predict the physiological information of oilseed rape under particulate matters pollution. In brief, the topic of this article mainly includes three parts. Firstly, get the spectral response characteristics of oilseed rape under the simulated particulate matters. Secondly, analyze the mechanism of oilseed rape leaf under particulate matters pollution based on ESEM. Thirdly, get the optimal method of inversion model of physiological information for oilseed rape. The amount of work we did is enormous, and the results show that this work is feasible and meaningful. The results could provide theoretical basis for the application of hyper-spectral technology in the response analysis of leafy vegetables under haze environment or particulate matters environment. The research could also provide reference for the management and physiological information monitoring of facility agricultural vegetables.

2 Materials and Methods

2.1 Objects and Methods

Oilseed rape, also known as *Brassica campestris L.*, is a Brassica of the cruciferous family. Oilseed rapes during four growing periods were selected as the object in this paper. Since spectral and physiological information measurement need to be carried out in clear and cloudless weather, the growth period of oilseed rape was postponed in abnormal weather such as cloudy and rainy days. And the final growing period was recorded as 16d, 25d, 32d and 48d respectively, which was expressed as “4-leaf age”, “4.5-leaf age”, “5-leaf age” and “5.5-leaf age” respectively in terms of leaf age. The seeds were purchased from Jilin Kefeng seed industry Co., Ltd., and then cultivated in the solar greenhouse of College of Biological and Agricultural Engineering, Jilin University, China. When three or four expanded leaves were on each oilseed rape plant, they were transplanted into plastic flowerpots with a diameter of 10 cm. Each flowerpot transplanted one oilseed rape to ensure enough growth space. In the soil for oilseed rape growth, the content of organic matter was 12.59 g/kg, total nitrogen of 0.727 g/kg, available phosphorus of 0.007 g/kg and available potassium of 0.15 g/kg.

As shown in Fig. 1, a particulate matters simulation transparent tent (90 × 40 × 60, cm) was customized using stainless steel pipe and PVC transparent film. Oilseed Rape grew in the experimental tent. A fan at the bottom was added to disperse the particulate matters more evenly. The grid shelf was added to make it easier for the flowerpots to move. The experimental tent was connected with the homemade PMMA particulate matters occurrence chamber (45 × 35 × 30, cm) through the control valve. The combustion materials in the chamber are composed of potassium nitrate, lactose, glue, ammonium chloride, crude anthracene and resin in a proportion of 6:4:1:3:2:1. The combustion products contain carbon oxides, nitrogen oxides, ammonium salts, nitrate, sulfate, metal ions, and smoke dust, etc. The recycling chamber was connected with the experimental tent. The combustion products were collected by the recycling chamber in order to protect our environment. Real-time aerosol monitors (Dust Trak DRX 8533, TSI, USA) was used to monitor particulate matters concentrations.

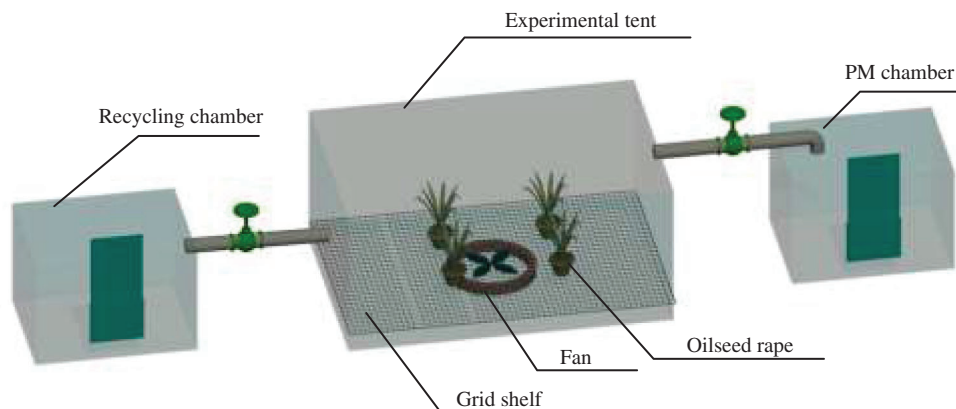


Figure 1: Testing apparatus components

Each test was divided into a control group (cg) and an experimental group (eg). The control group was healthy oilseed rape placed in the control tent (i.e., empty tent), and the experimental group was oilseed rape placed in the experimental tent under continuous influence of particulate matters. The air quality in the experimental tent was a serious pollution level. In Changchun, Jilin, the usual severe $PM_{2.5}$ concentration was about $250 \mu\text{g}/\text{m}^3$. It often happened during heating time. $500 \mu\text{g}/\text{m}^3$, which was two times $250 \mu\text{g}/\text{m}^3$ of Changchun was selected as the concentration of $PM_{2.5}$. Considering the labor and time cost, the concentration of $PM_{2.5}$ in the experimental group was maintained at $500 \mu\text{g}/\text{m}^3$. The purpose was also to get the obvious results [17]. The preliminary test showed that the spectrum in the experimental group would change significantly after 1 h. Combined with labor cost and the use time of instrument, the particulate matters exposure time was chosen for 1 h at last. But a 3 h particulate matters exposure experiment was also added to understand the mechanism better when we do microanalysis tests. In the experimental group, the soil was covered with plastic film in advance to eliminate the adsorption of soil and roots on particulate matters while the adsorption of plant stems was neglected [18]. In the study, ninety-six oilseed rapes during four different growing periods were investigated. Twenty-four oilseed rapes were tested in each growing period. On average, twenty-four oilseed rapes were put into six tents, of which three were the control tent, and the remaining three were the experimental tent. Each tent contained four oilseed rapes. Before the test, the concentrations of $PM_{2.5}$ and PM_{10} in the control tent were both $2 \mu\text{g}/\text{m}^3$, and the concentration of $PM_{1.0}$ was $1 \mu\text{g}/\text{m}^3$. The air quality index was excellent. Therefore, the particulate matter in the control tent was neglected. During the growth period, all oilseed rape had the same management conditions such as water, fertilizer and illumination, that is, the role of particulate matters was the only difference between the control and the experimental group.

To better reflect the physiological state of vegetation under special or stress environment, field surface reflectance in the range of two or more wavelengths was often combined for calculation, which is, using vegetation index (VI) to process spectral data for enhancing certain characteristics of vegetation and reflecting relevant indicators [19]. Studies showed that the NDVI index played an important role in the estimation of chlorophyll in plant leaves and had a good correlation with chlorophyll content and net photosynthetic rate [20]. NDVI, mNDVI705 and mSR705 were selected as sensitive spectral vegetation indices to analyze the effect of particulate matters on oilseed rape leaf in four growing periods. The vegetation indices were defined, as shown in Tab. 1.

Table 1: Formulas of spectral vegetation indices

| Vegetation indices | Definition | Calculation formula |
|--------------------|--|-------------------------------|
| NDVI | Normalized difference vegetation index | $(R815 - R715)/(R815 + R715)$ |
| mNDVI705 | Modified red edge normalized difference vegetation index | $(R815 - R550)/(R815 + R550)$ |
| mSR705 | Modified red edge simple ratio index | $(R750 - R445)/(R705 + R445)$ |

2.2 Data Collection and Processing

The experiment was conducted at 9:00–15:00 on sunny days from June to July, 2019, Beijing time (The experiment skipped rainy days and continued afterwards). And three functional leaves were taken to test for each of oilseed rape with the total amount of 288 leaves. All the data were repeated for three times and averaged as the data used in this study. Before the experiment, the functional leaves and oilseed rapes were marked. Hyper-spectral was measured by using Field Spec HandHeld 2 feature spectrometer (ASD company, U.S.) combined with probe equipped with a light source in the range of 325 nm~1075 nm. Sampling interval was 1.4 nm with a resolution of 3 nm @ 700 nm. Chlorophyll content was determined by SPAD-502 (Japan). Since the reading of SPAD-502 is closely related to chlorophyll content, its value is used to represent chlorophyll content in this paper [21]. Stomatal conductance was measured by a LI-6400 XT photosynthesizer (U.S.). ViewSpec Pro, SPSS 24.0 and Origin 19.0 were used for data processing and analysis. The principal component regression (PCR) is a dimension reduction modeling method which is commonly utilized in hyper-spectral image analysis. PCR uses a mathematical scheme to transform a set of highly correlated variables into a new set of uncorrelated principal components variables. This conversion reduces data redundancy [22]. The partial least square (PLS) can quickly treat huge data matrices of each object to extract the relevant part of the information and produce dependable models [23]. The chlorophyll content and net photosynthetic rate of oilseed rape leaf were the inversion variables in this study. The oilseed rape leaves in the collecting period were quickly cut with the area of 3 mm × 3 mm and flatly pasted on the metal sheet with conductive adhesive for microscopic observation. After gold spraying, using Environmental Scanning Electron Microscope (ESEM) (JEOL jsm-6700f, FEI company, USA) to observe the leaves and the microscopic images were analyzed.

3 Results and Discussion

3.1 Analysis of Spectral Characteristic Differences under the Effect of Particulate Matters

3.1.1 Effects of Particulate Matters on the Hyper-Spectral Characteristic

After obtaining the hyper-spectral data of healthy and particulate matters affected oilseed rape leaves in the four growing periods, Savitzky-Golay smoothing pretreatment with a window size of 10 was conducted on the original spectra to reduce the influence of background noise, obtaining the hyper-spectral curve as shown in Fig. 2. The most crucial waveband for monitoring plant growth and health was visible and near-infrared regions (400 nm~1075 nm). Within the range, the spectral curve trend of the control group and experimental group in Fig. 2 was almost the same. In the range of green light (490 nm~580 nm), the reflectance of oilseed rape was relatively high, showing “green mountain” peaks (reflection mountain at 550 nm), which was due to lowest utilization efficiency of green light of oilseed rape, causing the strongest reflection of green light. In the region of visible red light (620 nm~770 nm), the reflectivity value decreased first, and then it increased. Since the vegetation had the highest photosynthetic activity and absorbed most light in this region, it appeared “red valley” (reflection valley at 680 nm). In the short-wave near-infrared region (780 nm~1075 nm), the reflectance reached a stationary peak (a flattened slope from 780 nm) resulting from the reflection effect of mesophyll cells [24].

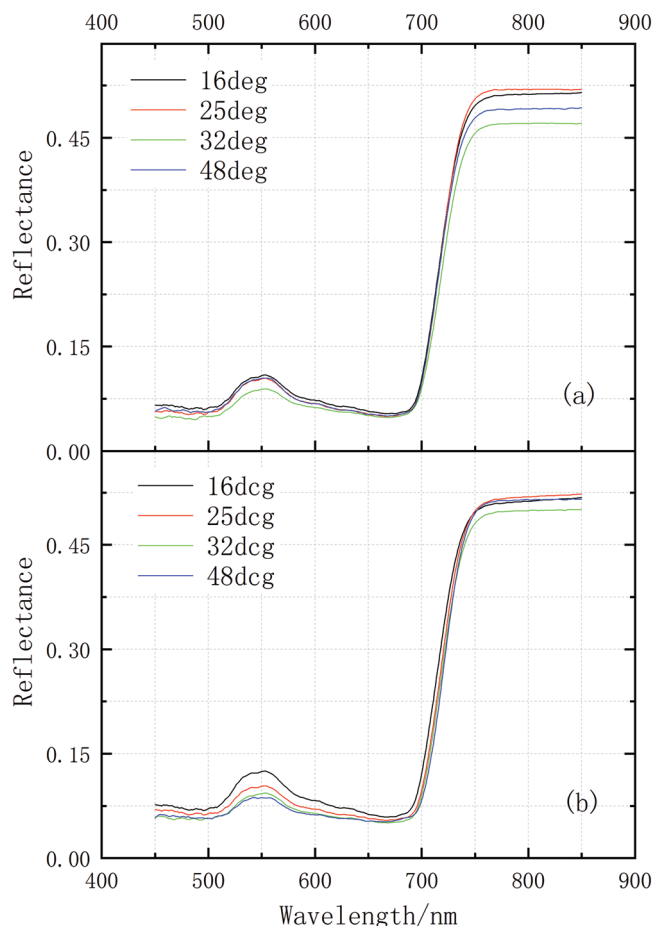


Figure 2: Hyper-spectral reflectance of oilseed rape in four growing periods under PM (eg) and non-PM (cg): (a) The experimental group (eg); (b) The control group (cg). Note: 16 d, 25 d, 32 d and 48 d: Four growing periods of oilseed rape; d: Growing days after transplant; eg: Experimental group; cg: Control group. The same below

Although the trend of the spectral curve was approximately the same, there are still differences between Figs. 2a and 2b. As shown in Fig. 2a, under the influence of particulate matters, the wave characteristics of hyper-spectral in the experimental group of various growing periods showed non-obvious change with slow changes of reflectivity in 500 nm~700 nm range. For oilseed rape in different growing periods, the “red valley” lowered and the reflection platform after 760 nm exhibited different heights [13]. For oilseed rape in the same period, the overall reflectance peak of the experimental group was lower than that of the control group except for the 48 d (collecting period) oilseed rape. The oilseed rape in collecting period showed higher reflectance value within the visible light region. The spectral reflectance value of leaf vegetables in the visible light range was mainly influenced by chlorophyll content. The oilseed rape leaf during the collecting period has the greenest color, and the chlorophyll content is the highest. The chlorophyll decomposed induced by particulate matters, so the content decreased the most, which reduced the light absorption of leaf most and increased the spectral reflectance. This is consistent with the results of previous studies: The reflectance of the diseased leaves in the area of loss of green becomes larger in the visible light range [25,26]. In the near infrared region of 760 nm~850 nm, the spectral reflectance of the experimental group and the control group in 16d and 25d growing periods were similar. On the other

hand, oilseed rape in 32 d and 48 d growing periods exhibited stronger resistance to the effect of particulate matters than those in younger leaf age. The damage degree of internal structure was lower, resulting in more light absorption and lower reflectivity of the experimental group than that of the control group.

3.1.2 Effects of Particulate Matters on First Derivative Spectral Characteristics

The characteristics of first derivative spectra of plants are closely related to physiological and ecological information, which can be used to describe the pigment state, health status and growing vitality of plants. The spectral “red edge” refers to the point where the slope of the reflection spectrum of the leaf is the largest in the range of red light (680 nm~760 nm) [27,28]. The spectral “red edge” is the most apparent spectral feature of green leaves and obtained by the maximum first-order derivative method in our research [29]. As shown in Fig. 3, the characteristics of the first derivative spectra of oilseed rape in different growing periods were different. The first derivative spectra of oilseed rape in different growing periods were compared respectively. Compared with the control group, the red edge of oilseed rape blue-shifted with various extents under the influence of particulate matters (except 16d), that is the position of red edge shifted to the direction of short wavelength. Moreover, with the increase of leaf age, the phenomenon of “blue shift” aggravated.

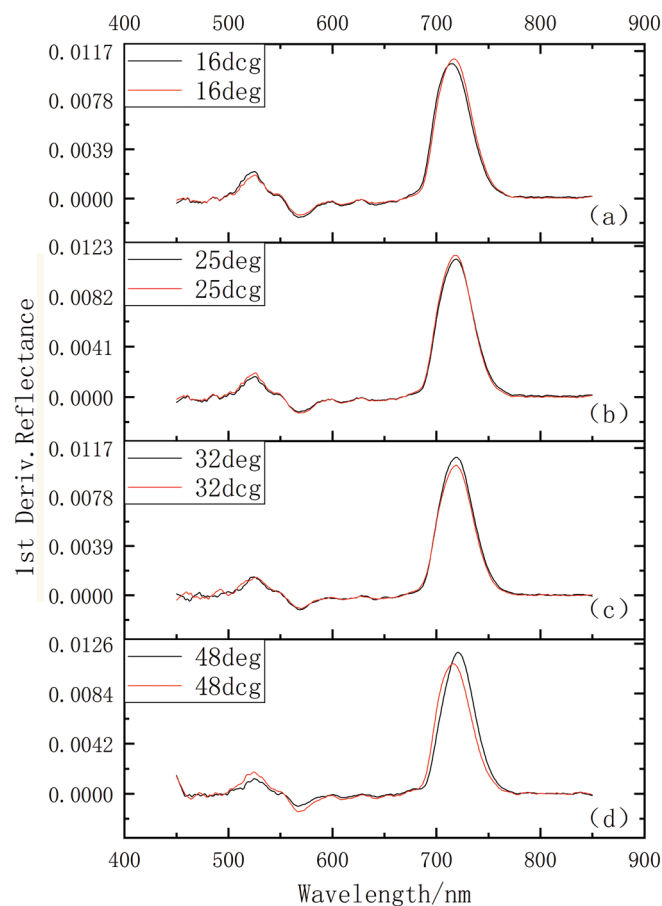


Figure 3: First derivative hyper-spectral characteristics of oilseed rape in four growing periods—(a)~(d) is 16d, 25d, 32d and 48d, respectively

From the observation of the naked eye, the oilseed rape leaf was smooth with relatively small surface area (the average area measured by leaf area meter was about 2427.5 mm²). Since the ability to retain particulate matters of the leaf with small area was weak, the leaf of oilseed rape had no advantage of resisting particulate matters, resulting in the apparent blue shift of red edge phenomenon that was observed in almost all growing periods [13]. As shown in Tab. 2, the red edge of oilseed rape blue shifted 1 nm, 1 nm and 8 nm for growing periods of 25d, 32d and 48d, respectively. The blue-shift of oilseed rape in the growing period of 48d was the most obvious. However, the red edge of oilseed rape in 16d red-shifted (3 nm), i.e., the position of red edge moved towards the direction of long wavelength. The position of the red edge could be used as an early warning indicator of the influence of particulate matters on leafy vegetables in the greenhouse, which could be used to diagnose the oilseed rape in combination with first derivative spectral characteristics.

Table 2: The red edge positions of oilseed rape in four growing periods

| Growing period (d) | Red edge position (nm) | |
|--------------------|------------------------|--------------------|
| | Control group | Experimental group |
| 16 | 714 | 717 |
| 25 | 719 | 718 |
| 32 | 720 | 719 |
| 48 | 722 | 714 |

The “yellow edge” of the spectrum was the maximum of first derivative reflectivity of yellow light between 560 nm~640 nm. The “blue edge” was the maximum of first derivative reflectivity of blue light between 490 nm~530 nm. It could be seen from Fig. 4 that the effect of particulate matters on yellow edge position was trivial. The yellow edge located near 628 nm. The amplitude of yellow edge increased showed the tendency of first increase and then decrease with the leaf age of oilseed rape. Such a trend was more obviously observed in the healthy leaves without the influence of particulate matters. Overall, particulate matters reduced the peak value of the yellow edge of oilseed rape leaf. Particulate matters had a little effect on the blue edge position of oilseed rape, which was near 525 nm. However, the amplitude of the blue edge showed a different trend. For healthy oilseed rape, the amplitude reduced with the increase of leaf age. On the other hand, the amplitude of the blue edge first increased, then decreased, and increased at last for oilseed rape affected by particulate matters. Overall, the amplitude of the blue edge decreased when subjected to particulate matters.

3.1.3 Effects of Particulate Matters on Sensitive Spectral Vegetation Index

With the growth of oilseed rape, the reflectance in 400 nm~700 nm of oilseed rape affected by particulate matters rose gradually, while the reduction of reflectance in 700 nm~900 nm aggravated gradually. The reflectance in the two regions were calculated by different methods, obtaining the vegetation index values for the experimental group and control group, as shown in Tab. 3. The variation trends of NDVI, mNDVI705 and mSR705 of oilseed rape of control group in four growing periods were consistent, all of which increased with the leaf age and reached the maximum in the 48d collecting period. The variation trends of the experimental group were different from that in the control group; however, the variation trends of the three vegetation indices were also consistent, all of which increased first and then decreased with the increase of leaf age. Meanwhile, the three vegetation indices achieved the lowest values in the 48d growing period. In general, the vegetation index values of the oilseed rape leaf in the experimental group were lower than that in the healthy control group due to the influence of particulate matters. The

variations of the three edge positions and the vegetation index could be used as the identification features of the response of oilseed rape to particulate matter.

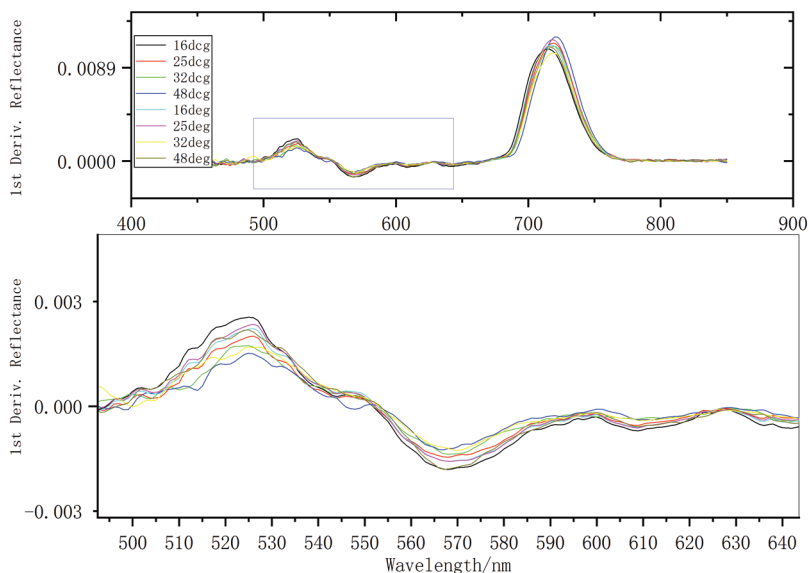


Figure 4: Zoomed first derivative spectral at 490 nm~640 nm

Table 3: Vegetation index values of oilseed rape in four growing periods

| Vegetation index | Group | Growing period (d) | | | |
|------------------|--------------------|--------------------|---------|---------|---------|
| | | 16 | 25 | 32 | 48 |
| NDVI | Experimental group | 0.34443 | 0.36159 | 0.36834 | 0.33792 |
| | Control group | 0.31004 | 0.37452 | 0.38000 | 0.42720 |
| mNDVI705 | Experimental group | 0.65311 | 0.66871 | 0.68516 | 0.64753 |
| | Control group | 0.61202 | 0.67052 | 0.68943 | 0.70963 |
| mSR705 | Experimental group | 2.00241 | 2.28439 | 2.27893 | 2.00126 |
| | Control group | 1.69978 | 2.06619 | 2.27365 | 2.38177 |

3.2 Response Mechanism of the Leaf to Particulate Matters Action

The deposition and adsorption of particle matter on oilseed rape leaf of 48 d growing period (the harvest period) were observed by Environmental Scanning Electron Microscope (ESEM). Figs. 5 and 6 compared the microstructure of healthy oilseed rape leaves and leaves affected by particulate matters for 1 h and 3 h. Fig. 5 showed that the surface of oilseed rape leaf presented the latticework shape, which had a specific advantage of capturing particulate matters. The surface of the healthy leaf (Fig. 5a) had less particulate matters, showing clear texture and evenly distributed bulging strips with apparent fluctuation. After 1 h under particulate matters environment (Fig. 5b), there were many fine and coarse particles on the surface of the leaf with more coarse particles near ridge stripe. After 3 h (Fig. 5c), more particles were stranded on the leaf surface, and some particles had gathered into clusters. As shown in Fig. 6, the stomata of the healthy leaf of oilseed rape were in the shape of the convex lens, with clearly observed outline of the stomata, large stomatal opening, and clearly ordered texture, showing no particulate matters

around. After 1 h under particulate matters environment, the stomatal opening became narrow, causing some particulate matters gathered into clusters around stomata. After 3 h, the deposited particulates around stomata increased. The texture distribution became disordered and stomata opening reduced more. The stomata were blocked by particulate matters, which crowded around the stomata in the shape of dentate or flake. It could be seen that the longer under the environment of particulate matters, the more particulates accumulated in the cells of oilseed rape leaf, which caused more significant damages to oilseed rape.

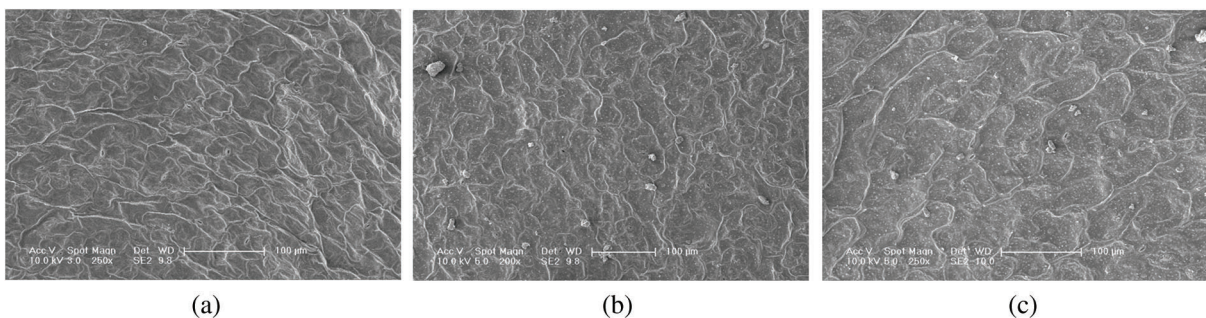


Figure 5: ESEM images of absorbed particulate matters on the surface of oilseed rape leaf– (a)~(c) is Healthy, PM influence for 1 hr. and PM influence for 3 hrs., respectively

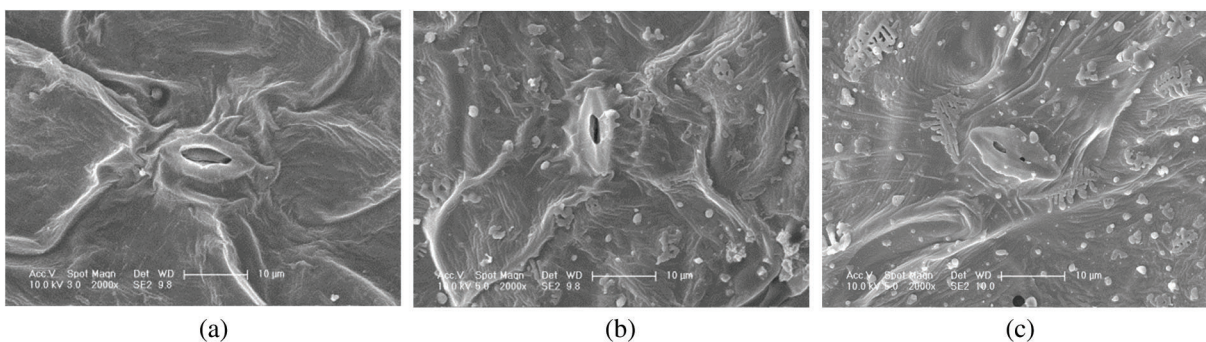


Figure 6: ESEM images of stomata on the surface of oilseed rape leaf– (a)~(c) is Healthy, PM influence for 1 hr. and PM influence for 3 hrs., respectively

Compared with the control group, the leaf of oilseed rape in the experimental group accumulated more particulate matters after putting in the particulate matters' environment. Meanwhile, the stomata changed significantly. With the prolonging of exposure to the particulate matters environment, the stomatal length-width ratio decreased, and the stomata appeared to shrink in different levels, showing microstructure differences that explained the differences of spectral characteristics mentioned above. Oilseed rape had its own protection mechanism, which would automatically narrow stomata slowly to reduce the harm of particulate matters after influenced by particulate matters. Nevertheless, invasive particulates still caused damages to the internal structure of the oilseed rape leaf. The degree of particulate matters damage to oilseed rape could be directly reflected through the change of stomatal length-width ratio. The length and width of stomata were measured using Digimizer v4.2.6. The mean value and the length-width ratio were calculated. The results showed that the stomatal length-width ratio of (a), (b) and (c) in Fig. 6 were 3.35, 2.83 and 2.13, respectively. It could be seen that the more serious the damage of particulate matter to rape leaves, the smaller the ratio of stomatal length to width.

The degree of the stomatal opening was usually expressed by stomatal conductance, which was the main factor influencing photosynthesis, respiration and transpiration of plants [13]. Many plants could reach the stomata opening of 4 μm ~6 μm , most of which were between 2.8 μm ~3.5 μm . Some plants had a larger opening of nearly nine μm , far larger than the diameter of fine particulate matters (2.5 μm). Therefore, fine particulate matters in the air could easily enter the leaf tissues of plants through stomata [30]. The subjects observed by ESEM above were oilseed rape leaves at 48 days during the harvest period. Similarly, the oilseed rape leaves during harvest period were selected to study stomatal conductance, as shown in Fig. 7. The average of stomatal conductance for the control group was about 0.182 $\text{mmol}\cdot\text{m}^{-2}\cdot\text{s}^{-1}$. However, the stomatal conductance of experimental group was generally higher than that of the control group, which was due to that particulate matters increased the stomatal conductance of oilseed rape in the collecting period.

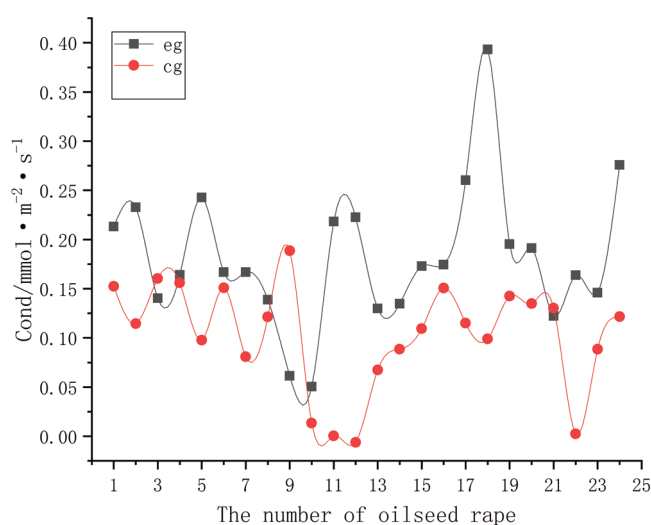


Figure 7: Comparison of stomatal conductance of oilseed rape under PM (eg) and non-PM (cg)

It would accelerate the senescence, damage and even necrosis of plants when plants were subjected to particulate matters pollution for a long time. Chlorophyll content and chlorophyll fluorescence parameters would decrease due to air pollution, while cell membrane permeability and non-photochemical quenching (qN) value would increase [31]. Fig. 6 showed that the stomatal opening of healthy oilseed rape could reach about seven μm , which allowed particulate matters to enter stomata, leading to the blockage of stomata of oilseed rape leaf. It was possible that particulate matters could destroy enzymes in the oilseed rape, which played an essential role in chlorophyll synthesis. Therefore, the chlorophyll content of oilseed rape leaf reduced, decreasing the photosynthetic ability of the photosynthetic system and affecting physiological processes such as photosynthesis and transpiration [32]. In this bad particulate matters environment, internal physiological processes of oilseed rape including stomatal closure happened, which reduced the involvement of particulate matters into the metabolism of plants through not entering mesophyll cells, lowering the damage [33,34]. However, the experimental results showed that the stomatal conductance of oilseed rape leaf in the collecting period increased not decreased. In the future, more experiments are needed to analyze how stomata in leaf adjusted the opening size according to the change of environment to reach the balance of physiological activities of plants [35].

3.3 Establishment of Inversion Model of Chlorophyll Content and Net Photosynthetic Rate

The change of the red edge of leaf spectrum was related to the variation of chlorophyll in leaves, and the red edge was positively correlated with chlorophyll content [36]. Besides, the photosynthetic carbon assimilation of the plant was carried out in chloroplast [37]. Meanwhile, some studies showed that the hyper-spectral characteristics of oilseed rape leaf were highly correlated with chlorophyll content and net photosynthetic rate [38–42]. With the aggravation of particulate matters pollution, the content of chlorophyll, and the chlorophyll fluorescence parameters (F_v/F_m , F_v/F_o , TPS II, qP) in leaves decreased [43]. The chlorophyll content and net photosynthetic rate of oilseed rape leaf changed because of particulate matters [5,34,44]. So, it was of great significance to investigate the inversion model of chlorophyll content and net photosynthetic rate for obtaining and analyzing the photosynthetic physiological information and spectral characteristics of oilseed rape under the influence of particulate matters.

Fig. 2 exhibited the reflectance peak of spectral in 510 nm~620 nm. With a clear curve and no overlapping, this range could better reflect the relation between chlorophyll content of oilseed rape and spectral characteristics. Therefore, the range of 510 nm~620 nm was selected as the sensitive wavebands of the spectrum to establish the inversion model of chlorophyll content (SPAD value) and net photosynthetic rate of oilseed rape leaf.

Three quarters of sensitive hyper-spectral data in 510 nm~620 nm range of oilseed rape leaf during the collecting period were randomly selected as the correction set and the remaining as the prediction set. The inversion model of chlorophyll content and net photosynthetic rate of oilseed rape affected by particulate matters during the collecting period was established respectively. In the process of modeling, the original hyper-spectral was processed with four pretreatment methods including first derivative (FD), second derivative (SD), Savitzky-Golay smooth (SG), multiple scatter correction (MSC) and standard normal variable transformation (SNV) [45]. Partial least square (PLS) and principal component regression (PCR) modelling methods were adopted to build the model. Correlation coefficient of calibration (R_c) and the correlation coefficient of prediction (R_p) were used to evaluate the performance of the model. The results of the different combination of pretreatment and modeling methods were shown in Tab. 4. By comparing the results of 16 combination methods, the combination of PCR + MSC + SD + SG was finally determined the optimal combination method for establishing the chlorophyll content inversion model. And the coefficient of the calibration was $R_c = 0.9585$ and $R_p = 0.9297$, respectively. The combination of PLS + MSC + FD + SG was the optimal method for establishing the net photosynthetic rate inversion model with R_c of 0.9043 and R_p of 0.8955, respectively. The results of the residual ($-2 < \text{residual value} < 2$) indicated that the model was stable. The deviation results of RMSEC and RMSEP was larger than that of standard models, suggesting that particulate matters pollution interfered the establishment of the model. The modeling results could accurately predict the chlorophyll content and net photosynthetic rate of oilseed rape, and provide a reference for future model modification of leafy vegetables under particulate matters pollution environment, which was more practical.

Table 4: Results of the different combination of pretreatment and modeling methods

| Modeling object | Modeling method | Pretreatment method | Rc | Rp |
|-------------------------|-----------------|---------------------|--------|--------|
| Chlorophyll content | PLS | SNV | 0.9098 | 0.9299 |
| | | MSC | 0.9117 | 0.9571 |
| | | MSC + FD | 0.9036 | 0.8544 |
| | | MSC + SD | 0.9298 | 0.8703 |
| | | FD + SG | 0.9040 | 0.8745 |
| | | SD + SG | 0.9789 | 0.8555 |
| | | MSC + FD + SG | 0.9014 | 0.8291 |
| | | MSC + SD + SG | 0.9213 | 0.9055 |
| | PCR | SNV | 0.8304 | 0.8576 |
| | | MSC | 0.8840 | 0.8705 |
| | | MSC + FD | 0.8976 | 0.8640 |
| | | MSC + SD | 0.9424 | 0.9607 |
| | | FD + SG | 0.9212 | 0.9194 |
| | | SD + SG | 0.8458 | 0.7489 |
| | | MSC + FD + SG | 0.9029 | 0.9139 |
| | | MSC + SD + SG | 0.9585 | 0.9297 |
| Net photosynthetic rate | PLS | SNV | 0.8945 | 0.8922 |
| | | MSC | 0.9041 | 0.8949 |
| | | MSC + FD | 0.9036 | 0.8756 |
| | | MSC + SD | 0.8952 | 0.8889 |
| | | FD + SG | 0.8752 | 0.8813 |
| | | SD + SG | 0.8454 | 0.8371 |
| | | MSC + FD + SG | 0.9043 | 0.8955 |
| | | MSC + SD + SG | 0.9012 | 0.8979 |
| | PCR | SNV | 0.7958 | 0.7943 |
| | | MSC | 0.8352 | 0.8298 |
| | | MSC + FD | 0.8853 | 0.8532 |
| | | MSC + SD | 0.9003 | 0.8854 |
| | | FD + SG | 0.8962 | 0.8891 |
| | | SD + SG | 0.8824 | 0.8295 |
| | | MSC + FD + SG | 0.8945 | 0.8940 |
| | | MSC + SD + SG | 0.8993 | 0.8845 |

4 Conclusions

In this study, oilseed rapes at four different growing periods were investigated in the simulated particulate matters environment. In combination of hyper-spectral technology and ESEM observation, the

response of hyper-spectral characteristics of the leaf to particulate matters was investigated in-depth. Under the influence of particulate matters, oilseed rape in different growing periods exhibited consistent features of no apparent fluctuation of spectral. The red edge obviously blue-shifted under the influence of particulate matters, along with the impact on the amplitudes of yellow edge and blue edge, all of which showing declined trend. The ratio of stomatal length to width was smaller than the healthy oilseed. The effect of particulate matters could be identified by the change of vegetation indices. The optimized inversion model of chlorophyll content and net photosynthetic rate could be used to predict the physiological information of oilseed rape under particulate matters pollution during the collecting period.

Funding Statement: This work was funded under the auspices of the National Natural Science Foundation for Young Scientists Fund (31801259), the National Natural Science Foundation for Young Scientists Fund (32001418) and the Science and Technology Development Project of Jilin Province (20200402015NC).

Conflicts of Interest: The authors declare that they have no conflicts of interest to report regarding the present study.

References

1. Kanniah, K. D., Beringer, J., Tapper, N. J., Long, C. N. (2010). Aerosols and their influence on radiation partitioning and savanna productivity in northern Australia. *Theoretical and Applied Climatology*, 100(3–4), 423–438. DOI 10.1007/s00704-009-0192-z.
2. Nguyen, T., Yu, X., Zhang, Z., Liu, M., Liu, X. (2015). Relationship between types of urban forest and PM_{2.5} capture at three growth stages of leaves. *Journal of Environmental Sciences*, 27(1), 33–41. DOI 10.1016/j.jes.2014.04.019.
3. Gao, G. J., Sun, F. B., Thao, N. T. T., Lun, X., Yu, X. (2015). Different concentrations of TSP, PM₁₀, PM_{2.5}, and PM₁ of several urban forest types in different seasons. *Polish Journal of Environmental Studies*, 24(6), 2387–2395. DOI 10.15244/pjoes/59501.
4. Dzierzanowski, K., Popek, R., Gawrońska, H., Saebø, A., Gawroński, S. W. (2011). Deposition of matter of different size fractions on leaf surfaces and in waxes of urban forest species. *International Journal of Phytoremediation*, 13(10), 1037–1046. DOI 10.1080/15226514.2011.552929.
5. Kong, L. J., Yu, H. Y., Chen, M. C., Piao, Z. J., Dang, J. M. et al. (2019). Effects of particle matters on plants: A review. *Phyton-International Journal of Experimental Botany*, 88(4), 367–378.
6. Hwang, H. J., Yook, S. J., Ahn, K. H. (2011). Experimental investigation of submicron and ultrafine soot particle removal by tree leaves. *Atmospheric Environment*, 45(38), 6987–6994. DOI 10.1016/j.atmosenv.2011.09.019.
7. Guo, L., Ma, S. L., Zhao, D. S., Zhao, B., Xu, B. et al. (2019). Experimental investigation of vegetation environment buffers in reducing particulate matters emitted from ventilated poultry house. *Journal of the Air & Waste Management Association*, 69(8), 6987–6994.
8. Wu, C. Y., Wang, X. F. (2014). Effects of foliar dust on plant reflectance spectra and physiological ecology: A review. *Chinese Journal of Applied & Environmental Biology*, 20(6), 1132–1138.
9. Perini, K., Ottel , M., Giulini, S., Magliocco, A., Roccotiello, E. (2017). Quantification of fine dust deposition on different plant species in a vertical greening system. *Ecological Engineering*, 100, 268–276. DOI 10.1016/j.ecoleng.2016.12.032.
10. Kong, W. W., Zhang, C., Cao, F., Liu, F., Luo, S. et al. (2018). Detection of sclerotinia stem rot on oilseed rape (*Brassica napus* L.) leaves using hyperspectral imaging. *Sensors*, 18(6), 1764. DOI 10.3390/s18061764.
11. Kong, W. W., Zhang, C., Huang, W. H., Liu, F., He, Y. (2018). Application of hyperspectral imaging to detect sclerotinia sclerotiorum on oilseed rape stems. *Sensors*, 18(2), 123. DOI 10.3390/s18010123.
12. Rumpf, T., Mahlein, A. K., Steiner, U., Oerke, E. C., Dehne, H. W. et al. (2010). Early detection and classification of plant diseases with Support Vector Machines based on hyperspectral reflectance. *Computers and Electronics in Agriculture*, 74(1), 91–99. DOI 10.1016/j.compag.2010.06.009.

13. Leonard, R. J., McArthur, C., Hochuli, D. F. (2016). Particulate matter deposition on roadside plants and the importance of leaf trait combinations. *Urban Forestry & Urban Greening*, 20, 249–253. DOI 10.1016/j.ufug.2016.09.008.
14. Sgrigna, G., Baldacchini, C., Esposito, R., Calandrelli, R., Tiwary, A. et al. (2016). Haracterization of leaf-level matter for an industrial city using electron microscopy and X-ray microanalysis. *Science of the Total Environment*, 548–549, 91–99. DOI 10.1016/j.scitotenv.2016.01.057.
15. Ram, S. S., Majumder, S., Chaudhuri, P., Chanda, S., Santra, S. C. et al. (2014). Plant canopies: Bio-monitor and trap for re-suspended dust particulates contaminated with heavy metals. *Mitigation and Adaptation Strategies for Global Change*, 19(5), 499–508. DOI 10.1007/s11027-012-9445-8.
16. White, J. C., Arnett, J. T., Wulder, M. A., Tompalski, P., Coops, N. C. (2015). Evaluating the impact of leaf-on and leaf-off airborne laser scanning data on the estimation of forest inventory attributes with the area-based approach. *Canadian Journal of Forest Research*, 45(11), 1498–1513. DOI 10.1139/cjfr-2015-0192.
17. Wen, X., Zhang, P. Y., Liu, D. Q. (2018). Spatiotemporal variations and influencing factors analysis of PM_{2.5} concentrations in Jilin Province, Northeast China. *Chinese Geographical Science*, 28(5), 810–822. DOI 10.1007/s11769-018-0992-0.
18. Przybysz, A., Sæbø, A., Hanslin, H. M., Gawroński, S. W. (2014). Accumulation of particulate matter and trace elements on vegetation as affected by pollution level, rainfall and the passage of time. *Science of the Total Environment*, 481, 360–369. DOI 10.1016/j.scitotenv.2014.02.072.
19. Chang, H. X., Cai, X., Chen, X., Sun, K. (2018). Response characteristics analysis of different vegetation indices to leaf area index of rice. *Spectroscopy and Spectral Analysis*, 38(1), 205–211.
20. Li, Z., Zhang, F., Chen, L. H., Zhang, H. W. (2018). Research on spectrum variance of vegetation leaves and estimation model for leaf chlorophyll content based on the spectral index. *Spectroscopy and Spectral Analysis*, 38(5), 1533–1539.
21. Peng, J., Xu, F., Deng, K., Wu, J., Li, W. et al. (2018). Spectral differences of tree leaves at different chlorophyll relative content in Langya Mountain. *Spectroscopy and Spectral Analysis*, 38(6), 1839–1849.
22. Asante, E. A., Du, Z., Lu, Y. Z., Hu, Y. G. (2020). Detection and assessment of nitrogen effect on cold tolerance for tea by hyperspectral reflectance with PLSR, PCR, and LM models. *Information Processing in Agriculture*, 3, 1–9.
23. Haaland, D. M., Thomas, E. V. (2002). Partial least-squares methods for spectral analyses. 1. Relation to other quantitative calibration methods and the extraction of qualitative information. *Analytical Chemistry*, 60(11), 1193–1202. DOI 10.1021/ac00162a020.
24. Sun, T. T., Lin, W., Li, Y., Guo, P., Zeng, Y. (2017). Effect of different dust weight levels on urban canopy reflectance spectroscopy. *Spectroscopy and Spectral Analysis*, 37(8), 2539–2545.
25. He, Y., Liu, F., Li, X. L., Shao, Y. N. (2016). *Spectroscopy and imaging technology in agriculture*. Beijing: Science Press.
26. Liang, S. Z., Shi, P., Ma, W. D., Xing, Q. G., Yu, L. C. (2010). Relational analysis of spectra and red-edge characteristics of plant leaf and leaf biochemical constituent. *Chinese Journal of Eco-Agriculture*, 18(4), 804–809. DOI 10.3724/SP.J.1011.2010.00804.
27. Li, Y. X., Chen, X., Luo, D., Li, B., Wang, S. et al. (2018). Effects of cuprum stress on position of red edge of maize leaf reflection hyperspectral and relations to chlorophyll content. *Spectroscopy and Spectral Analysis*, 38(2), 546–551.
28. Luo, D., Chang, Q. R., Qi, Y. B. (2019). Estimation of chlorophyll content in apple leaves based on red edge parameters and artificial neural network. *Journal of Northwest A & F University*, 47(1), 107–115.
29. Ding, Y. Y., Zhang, J. J., Li, X. H., Li, M. Z. (2016). Estimation of chlorophyll content of tomato leaf using spectrum red edge position extraction algorithm. *Transactions of the Chinese Society for Agricultural Machinery*, 47(3), 292–297.
30. Wang, Q. J. (2016). *Soil physics and crop growth models*. Beijing: China Water Resources and Hydropower Press.
31. Hirano, T., Kiyota, M., Aiga, I. (1995). Physical effects of dust on leaf physiology of cucumber and kidney bean plants. *Environmental Pollution*, 89, 255–261.

32. Zhou, L. N. (2014). *Identification and warning of rice leaf blast based on analysis of chlorophyll fluorescence spectrum (Ph.D. thesis)*. Jilin University, China.
33. Su, X., Hu, D. Q., Lin, Z. F., Lin, G., Kong, G. (2002). Effect of air pollution on the chlorophyll fluorescence characters of two forestation plants in Guangzhou. *Acta Phytoecologica Sinica*, 26(5), 599–604.
34. Darestaa, B. E., Italiano, F., Gennaro, G., Trotta, M., Tutino, M. et al. (2015). Atmospheric particulate matter (PM) effect on the growth of *Solanum lycopersicum* cv. Roma plants. *Chemosphere*, 119, 37–42.
35. Yeboah, A., Lu, J. N., Yang, T., Shi, Y. Z., Amoanimaa-Dede, H. et al. (2020). Assessment of castor plant (*Ricinus communis* L.) tolerance to heavy metal stress-A review. *Phyton-International Journal of Experimental Botany*, 89 (3), 453–472.
36. Dou, Z. G., Cui, L. J., Li, J., Zhu, Y., Gao, C. et al. (2018). Hyperspectral estimation of the chlorophyll content in short-term and long-term restorations of mangrove in Quanzhou Bay Estuary, China. *Sustainability*, 10(4), 1127.
37. Xue, L. H., Yang, L. Z. (2008). Comparative study on estimation of chlorophyll content in spinach leaves using various red edge position extraction techniques. *Transactions of the Chinese Society of Agricultural Engineering*, 24(9), 165–169.
38. Yang, J., Liao, G. P., Liu, F., Guan, C. Y. (2020). Prediction of chlorophyll content of rape leaves with hyperspectral imaging technology. *Journal of Agricultural Science and Technology*, 22(5), 86–96.
39. Wang, X. Q., Wang, F., Liao, G. P., Guan, C. Y. (2016). Multifractal analysis of rapeseed spectrum for chlorophyll diagnosis modeling. *Spectroscopy and Spectral Analysis*, 36(11), 3657–3663.
40. Ding, X. B., Liu, F., Zhang, C., He, Y. (2015). Prediction of SPAD value in oilseed rape leaves using hyperspectral imaging technique. *Spectroscopy and Spectral Analysis*, 35(2), 486–491.
41. Liu, C. (2019). *Remote estimation of leaf net photosynthetic rate using hyperspectral reflectance (M.S. Thesis)*. Wuhan University, China.
42. Jabbari, H., Gholamhosseini, M., Naeemi, M., Nasiri, A. (2018). Physiological response of early and late maturity oilseed rape cultivars to drought under two climate conditions. *Phyton-International Journal of Experimental Botany*, 87, 133–143.
43. Yue, X. J., Ling, K. J., Hong, T. S., Gan, H. M., Liu, Y. X. et al. (2018). Distribution model of chlorophyll content for Longan leaves based on hyperspectral imaging technology. *Transactions of the Chinese Society for Agricultural Machinery*, 49(8), 18–25.
44. Shao, F., Wang, L. H., Sun, F. B., Li, G., Yu, L. et al. (2019). Study on different matter retention capacities of the leaf surfaces of eight common garden plants in Hangzhou, China. *Science of the Total Environment*, 652, 939–951. DOI 10.1016/j.scitotenv.2018.10.182.
45. Guo, Z. M., Chen, Q., Zhang, B., Wang, Q., Ouyang, Q. et al. (2017). Design and experiment of handheld near-infrared spectrometer for determination of fruit and vegetable quality. *Transactions of the Chinese Society of Agricultural Engineering*, 33(8), 245–250.